MINISTERIO DE INDUSTRIA Y ENERGIA
SECRETARIA DE LA ENERGIA Y RECURSOS MINERALES

ANALISIS Y VALORACION DE LAS TECNICAS GEOFISICAS APLICADAS A LA INVESTIGACION GEOTERMICA

" A P E N D I C E II "

"Propiedades Físicas de los Sistemas Geotérmicos"

INSTITUTO GEOLOGICO Y MINERO DE ESPAÑA

Abril 1985

ANALISIS Y VALORACION DE LAS TECNICAS GEOFISICAS APLICADAS A LA INVESTIGACION GEOTERMICA

" A P E N D I C E II "

"Propiedades Físicas de los Sistemas Geotérmicos"

A.II.6

PROPIEDADES FISICAS DE LOS SISTEMAS GEOTERMICOS

II-A. Moskowitz, B., and Norton, D., 1977, A preliminary analysis of intrinsic fluid and rock resistivity in active hydrothermal systems: Jour. Geophysical Research, v. 82, p. 5787-5795.

II-B. Ward, S.H., and Sill, W.R., 1984, Resistivity, induced polarization, and self-potential methods in geothermal exploration: Univ. Utah Res. Inst., Earth Sci. Lab., Rept. DOE/ID/12079-90, ESL-108, (Chapter III - Electrical Properties of Earth Materials).

II-C. Sill, William R., Electromagnetic properties of rocks, unpublished manuscript.

A PRELIMINARY ANALYSIS OF INTRINSIC FLUID AND ROCK RESISTIVITY IN ACTIVE HYDROTHERMAL SYSTEMS

B. Moskowitz and D. Norton

Department of Geology and Geophysics, University of Minnesota, Minneapolis, Minnesota 54421
Department of Geosciences, University of Arizona, Tucson, Arizona 85721

Abstract. Electrical resistivity data are utilized in interpretations of subsurface environments and to explore for geothermal and mineral resources. Abnormally low resistivity data are alternatively interpreted to indicate the presence of high-temperature fluids or conductive minerals (metal sulfides) at depth, even though relative contributions of thermal, porosity, and fluid composition effects appear to be poorly known. An analysis of intrinsic rock resistivities, calculated electrical porosities, and two-dimensional heat and mass transfer computations indicates that the host rock resistivity distribution around igneous intrusives is directly related to the mode of dispersion of thermal energy away from the pluton. Comparisons between numerical results and field observations in geothermal areas indicate that resistivity values in the vicinity of thermal anomalies are a complex function of fluid circulation patterns, fluid composition, and the distribution of conductive minerals produced by the reaction between circulating fluids and rocks; therefore in many cases, low near-surface resistivity anomalies cannot be entirely accounted for by hot circulating saline fluids, and observations of high thermal gradients associated with low-resistivity anomalies are not unique indications of a high-energy geothermal resource at shallow crustal depths.

Introduction

The nature of rocks in the upper crust is often deduced from apparent electrical resistivity data. The relationship between these data and the intrinsic resistivities is poorly known, and therefore correlation of the electrical resistivity measurement of rocks with variations in rock and pore fluid properties is usually speculative. Although interpretations are based on resistivity data measured in deep drill holes and laboratory measurements on rocks and fluids, the correlation of laboratory measurements, even in well-controlled laboratory experiments, with rock properties has not been satisfying. Better understanding of this correlation would facilitate mapping subsurface conditions with the aid of electrical survey data and is particularly relevant in regions of active hydrothermal activity, where there is considerable interest in energy resources.

The electrical resistivity variations in upper crustal rocks have been inferred from various electrical methods. The results of these surveys indicate that average resistivity values in stable crustal regions range from 10^5 to 10^2 ohm m [Keller and Frischknecht, 1966; Keller et al., 1966]. An analysis of laboratory experimental data on the resistivity of fluid-saturated crustal rocks coupled with considerations of regional heat flow data predict similar ranges in resistivity to a 40-km depth [Brace, 1971]. Resistivity surveys in regions of geothermal activity indicate anomalously low resistivities, which range between 10 and 100 ohm m [Sato, 1970; Cheng, 1970; Risk et al., 1970; Zohdy et al., 1973; Keller, 1970]. These anomalous values are often attributed to the presence of prospective thermal energy resources.

The properties and conditions in geothermal systems which contribute to resistivity values are fluid and mineral composition, porosity, temperature, and pressure [Brace, 1971; Brace and Orange, 1968; Brace et al., 1965; Keller and Frischknecht, 1966]. The effect of porosity and fluid resistivity on the bulk rock resistivity of sedimentary rocks was deduced by Archie [1942] and extended to crystalline rocks by Brace et al. [1965]. The empirical relationship derived by Archie defines bulk rock resistivity ρ_r as

$$\rho_r = a\rho_f\phi^{-n} \qquad (1)$$

in terms of pore fluid resistivity ρ_f, a proportionality constant a, porosity ϕ, and a factor which depends on the degree of rock consolidation, n. Experimental data by Brace et al. [1965] and Brace [1977] suggest that for fractured media, $a = 1$ and $n = 2$, values which apparently agree with theoretical electrical network models of Greenberg and Brace [1969] and Shankland and Waff [1974]. The porosity value normally used in (1) is that of total rock porosity. However, only those pores which contribute to current flow should be included in this term, and in fractured media the total porosity is usually not totally composed of interconnected pores, as is indicated by studies of ion transport in these types of rocks [Norton and Knapp, 1977]. Ranges in rock resistivity of 6 orders of magnitude may be realized for reasonable variations in the abundance of interconnected pores in fractured media [Moskowitz, 1977].

The transient thermal history of rocks in hydrothermal systems related to cooling igneous bodies has been simulated, over large regions and for long time periods, by numerical methods [Norton and Knight, 1977]. Since the variation in resistivity of rocks relates directly to subsurface temperature and pressure conditions, their numerical models provide a basis with which to analyze intrinsic resistivity of hydrothermal systems. The purpose of this communication is to present the results of a first-order approximation to the nature of intrinsic resistivity in such systems. The study considered variations in permeability and porosity, heat sources, rock and fluid properties, including variation in pore fluid resistivity as a function of temperature, pressure, and concentration of components in solution, as well as the time

Paper number 7B0809.

dependence of these parameters in a two-dimensional domain.

Porosity

The distribution of porosity in the crust varies in response to changes in pore fluid pressure. Effective pressure P_e is the difference between confining pressure P_c and pore fluid pressure P_f:

$$P_e = P_c - P_f \tag{2}$$

The variation of effective pressure with depth in the crust shows that in many geologic environments, increases in pore fluid pressure, as a result of temperature increases, will cause the effective pressure to decrease [Knapp and Knight, 1977]. As a consequence of the low tensile strength of rocks, when effective pressure is reduced to zero, the rock will fracture. Thus an increase in porosity is expected at zero effective pressure.

The total porosity in fractured media may be represented by

$$\phi = \phi_F + \phi_D + \phi_R \tag{3}$$

where ϕ_F, the effective flow porosity represents those pores through which the dominant mode of fluid and aqueous species transport is by fluid flow, ϕ_D, the diffusion porosity, represents those pores through which the dominant mode of transport is by diffusion through the aqueous phase, and ϕ_R, the residual porosity, represents those pores not connected to ϕ_F or ϕ_D. Field observations and experimental studies indicate that ϕ_R apparently accounts for more than 90% of the total porosity observed in crystalline rocks at ambient conditions [Norton and Knapp, 1977]. Our studies indicate that when ϕ_R values are used in (1), intrinsic resistivities of saturated rocks are predicted reasonably well, whereas ϕ_F and ϕ_D predict values many orders of magnitude higher than observed values [Moskowitz, 1977].

The correlation between porosity values consistent with electrical diffusivity and ion diffusivity determined by Norton and Knapp [1977] is unclear. We have assumed that pore fluid thermal expansion in residual pores produces fractures which contribute to electrical porosity. The pore characteristics at which the fluid will simply flow from the pore in response to thermal expansion and not increase the porosity are considered to be typical of the flow porosity normally found in crystalline rocks. Therefore any increases in total porosity due to temperature occur approximately as the result of changes in residual porosity. These assumptions are justified by the fact that $\phi_R \gtrsim 0.9\phi$ and that ϕ is used in Archie's law. Residual porosity is certainly an upper limit to the actual electrical porosity of crystalline rocks, and subsequently, the intrinsic resistivity calculated from these assumptions represents minimum values. Also, conversion of residual porosity to flow or diffusion porosity which relates directly to permeability is not considered in the fluid flow models to be discussed below.

The concept presented by Knapp and Knight [1977] can be used to relate porosity change at zero effective pressure to temperature. The total derivative of the rock-pore volume at constant composition is

$$dV = \left(\frac{\partial V}{\partial T}\right)_P dT + \left(\frac{\partial V}{\partial P}\right)_T dP \tag{4}$$

where $V = V_r + V_f$, V_r is rock volume, and V_f is pore volume. The coefficients of isobaric thermal expansion α and isothermal compressibility β for the bulk rock are defined as

$$\alpha \equiv \frac{1}{V}\left(\frac{\partial V}{\partial T}\right)_P \tag{5a}$$

$$\beta \equiv -\frac{1}{V}\left(\frac{\partial V}{\partial P}\right)_T \tag{5b}$$

Substitution of (5a) and (5b) into (4) defines the total volume change in terms of α and β:

$$dV = V\alpha\, dT - V\beta\, dP \tag{6}$$

This total derivative can also be expressed in terms of the individual thermal expansions and compressibilities of pore fluid and rock:

$$dV = \left[V_f\alpha_f + V_r\alpha_r\right] dT - \left[V_f\beta_f + V_r\beta_r\right] dP \tag{7}$$

However, when rocks fracture as a consequence of pore fluid expansion, infinitesimal increases in pore fluid pressure will produce further fracturing. Therefore $dP \cong 0$, and (7) may be simplified to

$$dV = \left[V_f\alpha_f + V_r\alpha_r\right] dT \tag{8}$$

Typical values for α_r, for common silicate minerals, over a temperature range of 0°-800°C, are of the order of 10^{-6} °C^{-1} [Clark, 1966]. The thermal expansion coefficient for pure water, over the same temperature span, is of the order of 10^{-3} °C^{-1}. As long as pore volume V_f is greater than or equal to 0.01, $V_f\alpha_f >> V_r\alpha_r$, and (8) becomes

$$dV = V_f\, \alpha_f\, dT \tag{9}$$

The total volume change, according to (9), occurs as a result of pore volume changes, the rock volume remaining essentially constant. Rearranging (9) with the approximation that $dV \cong dV_f$ yields an integral equation relating pore volume and temperature:

$$\int_{V_f^o}^{V_f} \frac{dV_f}{V_f} = \int_{T_b}^{T} \alpha_f(T)\, dT \tag{10}$$

In (10), V_f^o is the initial residual pore volume, and T_b is the temperature at which the rock fractures. Integrating (10) gives the pore volume as a function of temperature:

$$V_f = V_f^o \exp\left[\int_{T_b}^{T} \alpha_f(T)\, dT\right] \quad (11)$$

where $T > T_b$. The initial residual porosity ϕ_R^o is defined as

$$\phi_R^o = \frac{V_f^o}{V^o} = \frac{V_f^o}{V_r + V_f^o} \quad (12)$$

and the fluid and rock volumes are

$$V_f^o = \phi_R^o V^o \qquad V_r = (1 - \phi_R^o)V^o \quad (13)$$

respectively. Substituting (12) and (13) into (11) defines a porosity temperature function in terms of the initial residual porosity:

$$\phi_R = \frac{\phi_R^o F(T)}{(1 - \phi_R^o) + \phi_R^o F(T)} \quad (14)$$

where

$$F(T) = \exp\left[\int_{T_b}^{T} \alpha_f(T)\, dT\right] \quad (15)$$

For the purposes of this discussion we will consider that (14) defines increases in the effective electrical porosity. That is, all porosity increases due to thermal effects are assumed to contribute to increased electrical current flow in the rocks.

The temperature at which the rocks initially fracture, T_b, may be defined as

$$T_b = T_a + \Delta T \quad (16)$$

where T_a is the ambient temperature and ΔT is the temperature increment necessary to reduce effective pressure to zero. The value of ΔT depends on the geothermal gradient, and the maximum value of ΔT along a gradient of 20°C/km is 20°C [Knapp and Knight, 1977].

Porosity, defined by (14), was computed for depths of 1, 2, 3, and 4 km below the earth's surface (Figure 1). At a depth of 1 km and initial temperature of 40°C, large increases in porosity are predicted for temperature changes of the order of 300°C. However, the porosity increases are small for changes in temperatures of less than 100°C at this same depth. At greater depths, e.g., 4 km, much smaller increases in porosity are predicted for these same temperature conditions, owing to increased confining pressure.

The relationship among bulk rock resistivity, fluid resistivity, and electrical porosity is

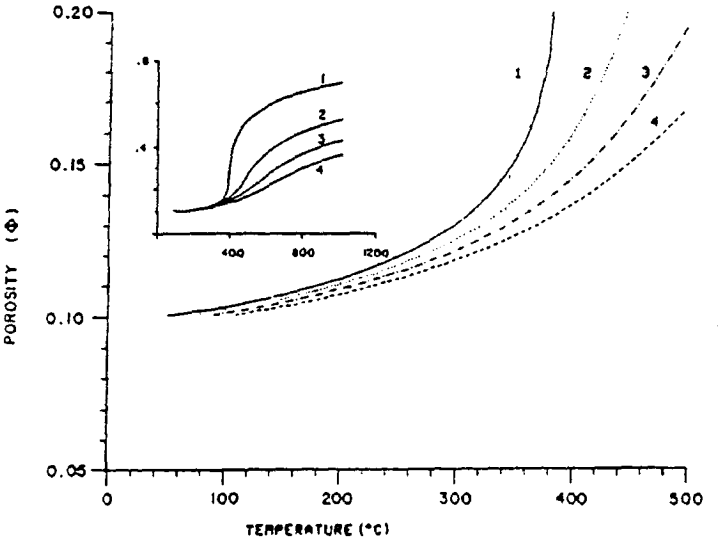

Fig. 1. Porosity as a function of temperature at depths of 1, 2, 3, and 4 km, as computed from (14). Initial porosity ϕ_o is 0.1, and background temperatures are consistent with a surface temperature of 20°C and a temperature gradient of 20°C/km. Pressures were computed for a rock density of 2.75 g/cm^3. Insert shows porosity values consistent with temperatures up to 1200°C.

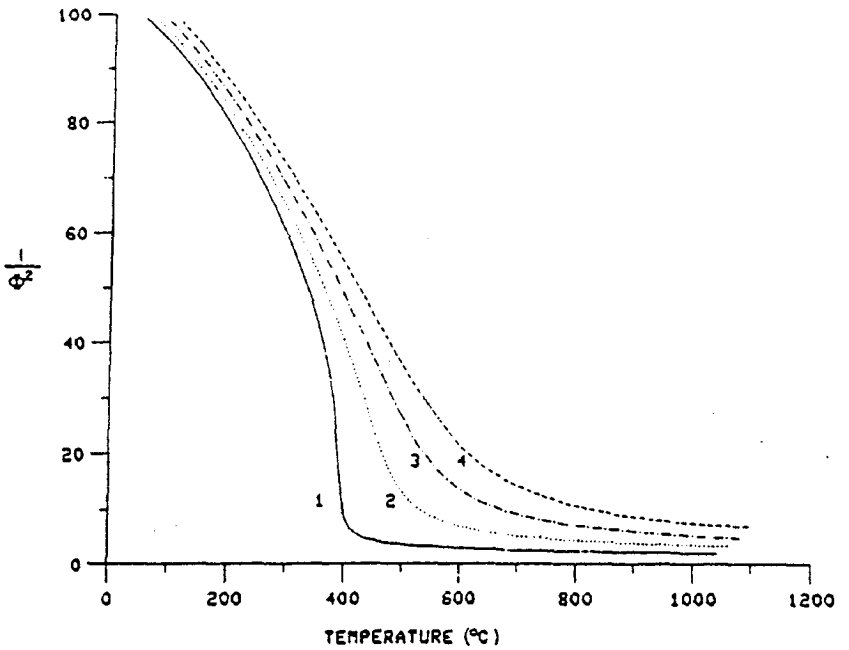

Fig. 2. Parameter ϕ^{-2} as a function of temperature at depths of 1, 2, 3, and 4 km. Parameters used are same as those in Figure 1.

poorly known. Archie's law, equation (1), has been assumed as an adequate first approximation to rock resistivity. Therefore the important parameter in predicting resistivity from (1) is ϕ^{-2}, and therefore small increases in porosity will result in a significant decrease in ρ_R (Figure 2).

Fluid Resistivity

The resistivity of natural groundwaters varies as a function of temperature, pressure, and composition. Since the dissolved constituents in natural waters are often dominated by sodium and chloride, and the resistivity values of NaCl-H_2O fluids are similar, within a factor of 2.5, to those of other common fluids, the compositional effects of fluid resistivity are approximated by the system NaCl-H_2O [Quist and Marshall, 1968; Chambers, 1957; Gunning and Gordon, 1942]. The variation in resistivity of a 0.1 m NaCl solution with temperature and pressure exhibits a steady, pressure independent decrease in resistivity to approximately 300°C, then an order of magnitude increase to 12 ohm m at 500°C and 500 bars (Figure 3). As can be seen, the dominant pressure effect is to shift the resistivity minimum to higher temperatures with increasing pressure. Increasing the NaCl concentration results in a decrease in resistivity that varies from 100 to 0.01 ohm m for concentrations ranging from 10^{-4} to 2 m.

Fluid temperatures in geothermal reservoirs range up to 300°C, and pressures to 1 kbar. Total ionic strength of these fluids ranges from 1 m, such as was observed in the Imperial Valley system [Meidav and Furgerson, 1972] to 10^{-2} m, such as was observed in the Broadlands, New Zealand, system [Browne and Ellis, 1970]. Typical resistivities of geothermal reservoir fluids range from 0.01 to 10 ohm m [Cheng, 1970], which is similar to the range in resistivity of pore fluids in a variety of geologic environments [Keller and Frischknecht, 1966].

Temperature-Pressure Distribution

Notions of temperatures and pressures in geothermal systems are primarily derived from production or exploration wells, and consequently, information is restricted to small portions of the total system. Knowledge of these parameters over the entire hydrothermal system is necessary in order to analyze the time dependence of resistivity in the region of a cooling pluton. Simulation of cooling plutons by numerical methods is one method by which these parameters can be defined for an idealized geothermal system.

Fluid flow caused by thermal anomalies related to igneous plutons is effectively scaled and represented in two dimensions by partial differential equations which describe the conservation of mass, momentum, and energy for the fluid-rock system [Norton and Knight, 1977]:

Conservation of energy

$$\gamma \frac{\partial T}{\partial t} + q\nabla H = \nabla \cdot \kappa \nabla T \qquad (17)$$

Conservation of momentum

$$\frac{\nabla \cdot \upsilon \nabla \Psi}{k} = R \frac{\partial \rho}{\partial y} \qquad (18)$$

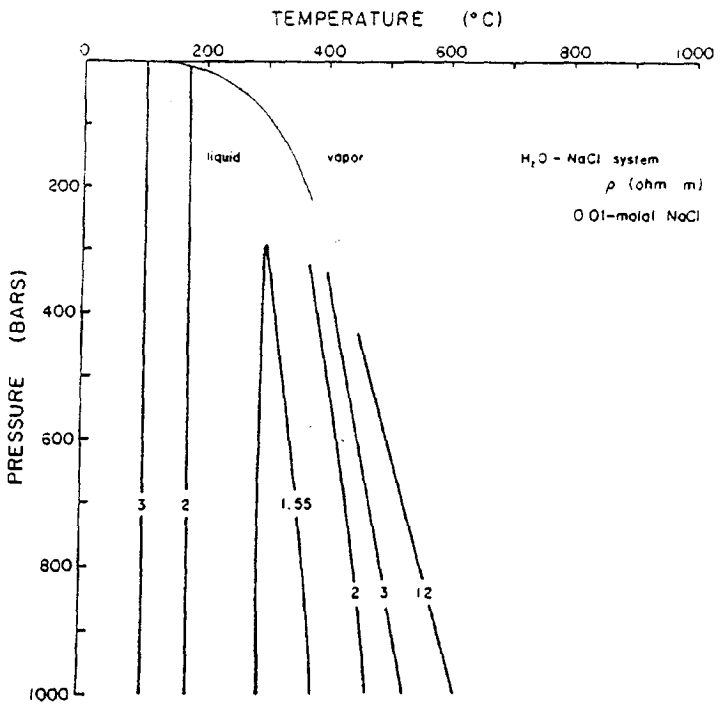

Fig. 3. Temperature-pressure projection of the two-phase surface (liquid and vapor) in the H_2O-NaCl system at 0.01-m NaCl concentration depicting fluid resistivity isopleths.

where T is the temperature, Ψ is the stream function, q is the fluid flux, t is the time, H, ρ, and ν are the enthalpy, density, and viscosity of the fluid, k is the permeability of the rock, κ is the thermal conductivity, and γ is the volumetric heat capacity of the fluid-saturated media, R is the Rayleigh number, ∇ is the gradient operator, and y is the horizontal distance in the two-dimensional section to which these equations apply.

Equations (17) and (18) are approximated by finite difference numerical equations which permit computation of the values of the dependent variables at discrete points in the domain from initial and boundary values specified for the system. The numerical analysis provides the option to include variable transport properties of the fluid (H_2O system) and rock, general boundary and initial conditions, and radioactive and volumetric heat sources in a two-dimensional domain. The transport process related to the transient thermal anomaly is approximated by a time sequence of steady state numerical solutions to (17) and (18), computed at explicitly stable time intervals. An alternating direction implicit finite difference method is used to approximate the spatial derivatives at discrete intervals of the order of 0.1-0.5 of the system height. Fluid pressure in the system is computed at each steady state step by integration of Darcy's law, in which the fluid properties, viscosity and density, are expressed as a function of temperature and pressure.

The methods used by Norton and Knight [1977] were used to define the temperature variation in the environment of a cooling pluton as a function of time. The hypothetical system is characterized by a dominance of convective heat transport over conductive heat transport as a result of relatively large host rock permeabilities (Figure 4). As a consequence of fluid circulation the temperature distribution in the host rocks evolves into a plumose pattern at $\sim 10^5$ years (Figure 5) and results in broad regions of uniform temperature above the pluton.

Initial temperatures in the host rocks at this depth are 110°C, as defined by the 20°C/km geothermal gradient and 20°C surface temperature. At 190,000 years after pluton emplacement the 200°C isotherm is at approximately a 0.5-km depth (Figure 5), and the temperatures between the top of the pluton and the 200°C isotherm have increased by at least 90°C. The pore fluid resistivity reaches a minimum at temperatures between 200°C and 300°C (Figure 3), and the porosity increase defined by (14) is of the order of 15% of the initial value for temperature increases of 100°-200°C. Therefore the zone between the 200°C isotherm and the top of the pluton in the system will be characterized by maximum porosity increase and the maximum decrease in pore fluid resistivity.

Porosities in host rocks at depths of <2 km directly over the pluton have significantly increased approximately 20% of the initial value at 190,000 years after pluton emplacement. This porosity increase persists uniformly to a 4-km depth. Time variations in porosity, calculated

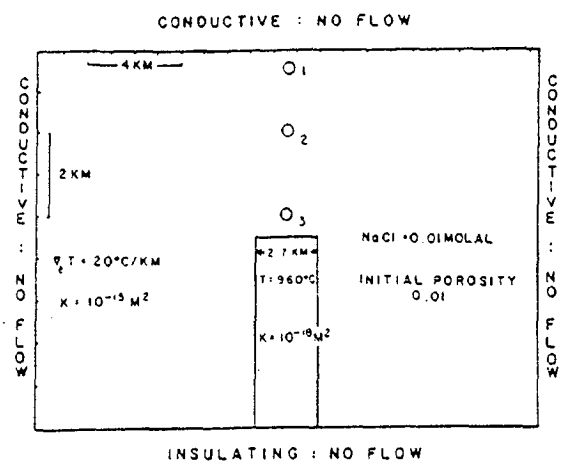

Fig. 4. Two-dimensional cross section of a pluton intruded into uniform permeability host rocks depicting initial and boundary conditions for numerical simulation of heat and mass transfer. Domain was discretized into 120 grid points such that $\Delta z = 0.9$ km and $\Delta y = 1.75$ km. The initial conditions include a background temperature consistent with a surface temperature of 20°C and a thermal gradient $\nabla_z T = 20°C/km$. The pluton's initial temperature is 960°C. Permeabilities are 10^{-15} m^2 and 10^{-18} m^2 for the host and pluton rocks, respectively.

at fixed points 4, 2.5, and 0.5 km above the top of the pluton, predict a maximum 0.5 km above the pluton at 4×10^4 and 10^5 years after emplacement (Figure 6). However, as a result of convective transport of thermal energy to the surface a porosity maximum is observed at depths of <2 km.

The spatial and temporal distribution of temperature in the system will directly determine the host rock resistivity distribution. The resistivity isopleths closely parallel the isotherms at 50,000 and 190,000 years (Figures 7 and 8, respectively), which also illustrate the displacement in the resistivity isopleths between 50,000 and 190,000 years. By 190,000 years the lateral extent of the isopleth displacement at a 1-km depth spans the entire width of the system (~22 km).

In summary, the calculations indicate that the dispersion of thermal energy away from a pluton will directly affect the host rock resistivity. When pluton emplacement is into permeable host rocks, significant decreases in resistivity between the surface and depths of <0.5 km are predicted. These resistivity values then persist uniformly in a vertical zone, extending from 0.5 km to approximately 4 km above the pluton by 190,000 years after pluton emplacement. The maximum decrease in resistivity is less than a factor of 10, as compared to surface values. The range in host rock resistivity is from 10^4 to 10^5 ohm m. These values are quite high with respect to values obtained on real rocks. However, our calculations only account for a conductive fluid in a nonconductive matrix.

Discussion

The temperature variations in hydrothermal systems account for changes in electrical porosity and electrical resistivity of pore fluids. Results of our analysis suggest that resistivity anomalies caused by thermal events are several times broader in extent than the thermal source, and the lateral resistivity gradients at the margins of the anomaly are much lower than the vertical resistivity gradients directly above the pluton. The side and top margins of the resistivity anomaly correspond closely to the 200° isotherm, as a consequence of the fluid properties. A resistivity minimum occurs at relatively shallow depths, e.g., 0.5 km, and extends to 4 km. However, the magnitude of these resistivities is considerably greater than values measured in geothermal systems.

The magnitude of ρ_R is defined by the pore fluid concentration and initial host rock porosity, while the distribution of ρ_R is defined by the temperature distribution. To determine the change in magnitude of ρ_R, due to varying molality of pore fluids and host rock porosities, a series of calculations was made with different initial values of porosity and NaCl molalities. The isopleths of resistivity as a function of porosity and NaCl molality at constant temperature are defined by (1) and shown for T = 300°C in Figure 9. The results of the calculations summarized as the minimum resistivities predicted for the cooling pluton environment are comparable to actual values realized in geothermal systems and in saline groundwater systems. In order to explain the observed resistivities in geothermal areas (<10 ohm m), high-molality pore fluids and/or high-porosity host rocks must occur for large vertical and horizontal zones within the geothermal system.

The results of this study indicate that rock resistivities characteristic of active hydrothermal systems are considerably less than can be accounted for by simple changes in fluid resistivity or rock porosity. The discrepancies be-

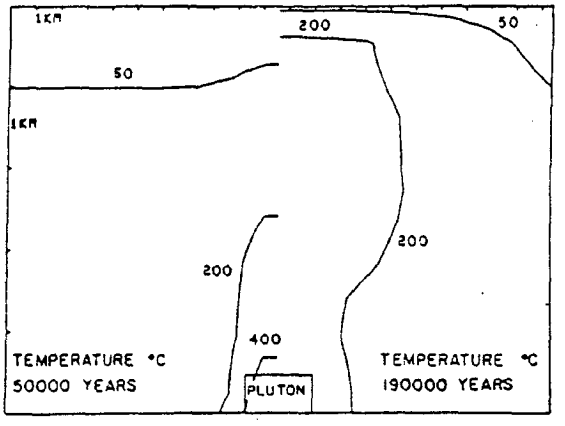

Fig. 5. Temperature distribution in an idealised hydrothermal system, defined by Figure 4, for (left) 5×10^4 and (right) 1.9×10^5 years elapsed time.

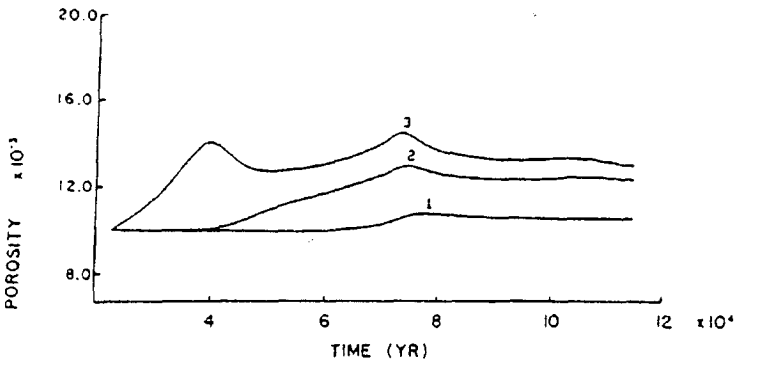

Fig. 6. Porosity as a function of time resulting from thermal energy transport into host rocks from the pluton at positions directly over the pluton, 0.5, 2, and 4 km below the surface (Figure 4).

tween the numerical resistivity models and the field resistivity observations in geothermal systems may be accounted for by the presence of conducting minerals, since pyrite and conductive clay minerals are typically found in the region of hydrothermal systems over the top of the thermal anomaly. If one uses a conservative estimate of a factor of 10 decrease in host rock resistivities resulting from conducting minerals, a geologically reasonable range in porosity and fluid composition can produce the anomalously low resistivity values observed in geothermal areas. Therefore except in anomalously high salinity and high porosity environments the presence of hot fluids alone is not sufficient to generate the low resistivity values observed in geothermal areas.

Considerable interest has been given to exploration techniques that might be useful in detecting high-energy geothermal systems. Commonly used techniques include measurements of heat flow and electrical resistivity. High heat flow in combination with anomalously low electrical resistivity data have been used as a justification for drilling of exploratory wells. Sedimentary basins and young, old, and mature geothermal systems in fractured rocks constitute a set of geologic environments within which the correlation of high thermal gradients, low near-surface resistivities, and surface thermal effects may lead to nonunique interpretations of the potential for geothermal energy resources at moderate depths. In the basin and range province of the western United States, concentrated brines associated with evaporite deposits in the high-porosity basins can produce lateral density gradients which cause fluid circulation. Exothermal hydration reactions that produce local thermal anomalies, coupled with the fluid circulation, are often sufficient to cause high surface heat flux and surface thermal springs. The high salinity and high porosity in these sedimentary basins would result in anomalously low near-surface resistivity. This particular environment appears

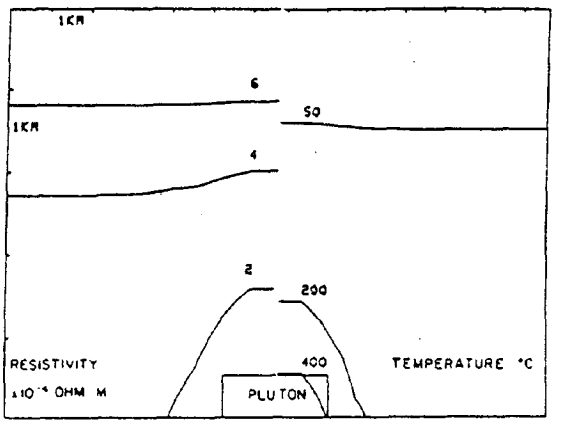

Fig. 7. Resistivity and temperature values in a hydrothermal system at 5×10^4 years elapsed time, depicting the temperature control on intrinsic resistivities.

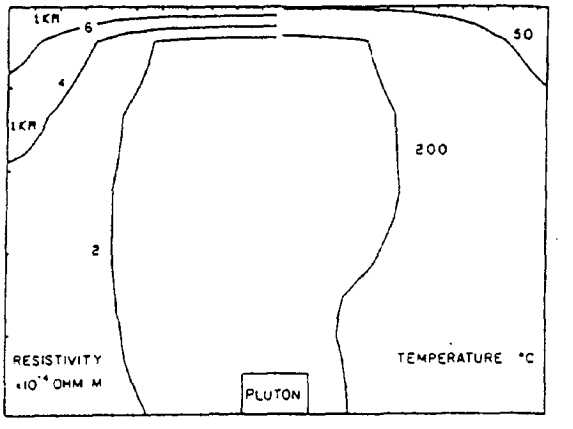

Fig. 8. Resistivity and temperature values in a hydrothermal system at 1.9×10^5 years elapsed time, depicting the temperature control on intrinsic resistivities.

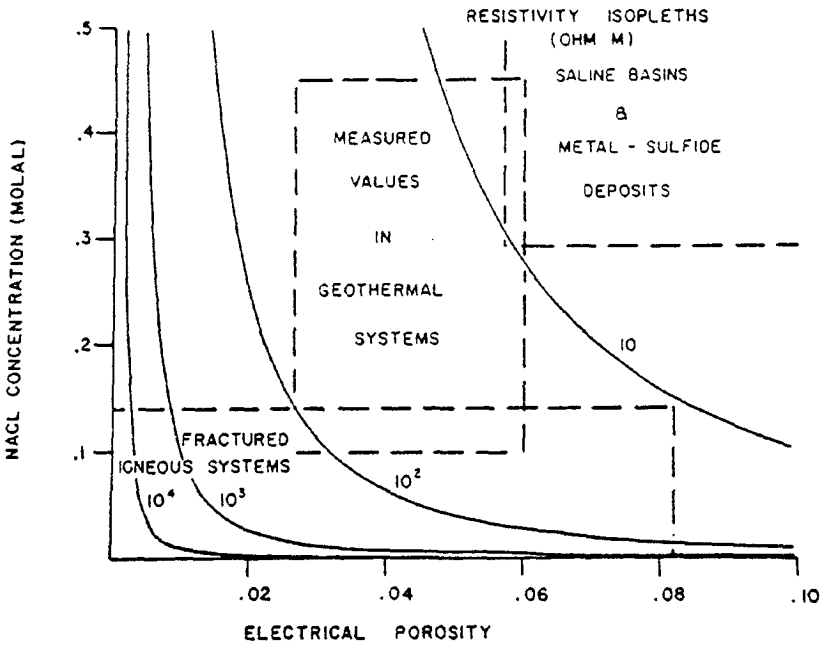

Fig. 9. Concentration of NaCl in pore fluids and electrical porosity effect on intrinsic rock resistivities, with isopleths of 10, 10^2, 10^3, and 10^4 ohm m. Values are for T = 300°C, at which the minimum in fluid resistivity occurs, and for P = 500 bars. Note that the minimum in fluid resistivity is nearly independent of pressures (Figure 3). Regions delimited by dashed lines represent ranges in values of porosity and fluid compositions observed in the respective geologic environments and for idealised systems considered in this study. The latter are labeled 'fractured igneous systems.'

to occur in the Safford Basin, southeastern Arizona [Norton et al., 1975].

Geothermal systems which have nearly cooled to regional background temperatures may be characterized by large conductive heat fluxes [Norton, 1977] as a result of remnant thermal energy that has been transported from the heat source to near-surface environments. Conducting minerals will undoubtedly have been formed above the pluton, and thermal springs will still be prevalent on the surface. In this environment, low resistivity would be associated with the conducting minerals and, in part, with the circulating saline fluids.

Geothermal systems in their early stages of formation have not been studied; however, their characteristics have been numerically simulated. The transport of thermal energy away from a pluton may be rapid with respect to the mass flux of reactive components in solution to the surface. This means that hot saline fluids will dominate changes in host rock resistivities because not enough time has elapsed to produce significant quantities of conducting minerals. High heat flux and surface thermal effects will probably form relatively early in the life cycle of a geothermal system. The calculated resistivity values resulting from increased temperatures are anomalous with respect to background values but are relatively high (10^4-10^5 ohm m). Therefore this environment is characterized by high heat flux and thermal surface effects but probably an undetectable resistivity anomaly, even though there is a high-energy thermal source at depth.

Active, mature geothermal systems are abundant worldwide where high heat flux, thermal surface effects, and low resistivities are associated with a productive thermal source at depth. However, low-resistivity anomalies, <100 ohm m, are probably caused by the presence of conductive minerals which may be coincident with hot thermal fluids.

The four geologic environments presented serve to illustrate the problems which can be encountered in attempting to interpret near-surface resistivity anomalies. Also a combination of heat flux measurements, surface thermal effects, and low resistivity can be characteristic of both productive high-energy geothermal systems and unproductive low-energy geothermal environments. The observations are also manifested in that electrical methods are used in prospecting for both sulfide mineral deposits and thermal energy.

Acknowledgments. We wish to acknowledge the Energy Research Development Administration for support of this study through contract E-11-1-2763. We thank Robert F. Butler, R. Knapp, and J. Knight for discussions and penetrating questions, L. McLean for editing and typing the manuscript, and the University Computer Center personnel for their assistance.

References

Archie, G. E., The electrical resistivity log as an aid in determining some reservoir characteristics, Trans. AIME, 146, 54-62, 1942.

Brace, W. F., Resistivity of saturated crustal rocks to 40 km based on laboratory studies, in The Structure and Physical Properties of the Earth's Crust, Geophys. Monogr. Ser., vol. 14, edited by J. G. Heacock, pp. 243-257, AGU, Washington, D. C., 1971.

Brace, W. F., Permeability from resistivity and pore shape, J. Geophys. Res., 82, 3343-3349, 1977.

Brace, W. F., and A. S. Orange, Further studies of the effect of pressure on electrical resistivity of rocks, J. Geophys. Res., 73, 5407-5420, 1968.

Brace, W. F., A. S. Orange, and T. R. Madden, The effect of pressure on the electrical resistivity of water-saturated crystalline rocks, J. Geophys. Res., 70, 5669-5678, 1965.

Browne, P. R. L., and A. J. Ellis, the Ohaki-Broadlands hydrothermal area, New Zealand: Mineralogy and related geochemistry, Amer. J. Sci., 269, 97-131, 1970.

Chambers, J. F., The conductance of concentrated aqueous solutions of potassium iodide at 25°C and of potassium and sodium chlorides at 50°C, J. Phys. Chem., 62, 1136, 1958.

Cheng, W. T., Geophysical exploration in the Tatun volcanic region, Taiwan, Geothermics, Spec. Issue, 2 (1), 910-917, 1970.

Clark, S. P. Jr., ed., Handbook of Physical Constants, Geol. Soc. America, Mem. 97, New York, Revised edition.

Greenberg, R. J., and W. F. Brace, Archie's law for rocks modeled by simple networks, J. Geophys. Res., 74, 2099-2101, 1969.

Gunning, H. E., and A. R. Gordon, The conductance and ionic mobilities for aqueous solutions of K and NaCl at T = 15°C-45°C, J. Chem. Phys., 10, 1942.

Keller, G. V., Induction methods in prospecting for hot water, Geothermics, Spec. Issue, 2 (1), 318-332, 1970.

Keller, G. V., and F. C. Frischknecht, Electrical Methods in Geophysical Prospecting, Pergamon, New York, 1966.

Keller, G. V., L. A. Anderson, and J. I. Pritchard, Geological survey investigations of the electrical properties of the crust and upper mantle, Geophysics, 31, 1078-1087, 1966.

Knapp, R., and J. Knight, Differential thermal expansion of pore fluids: Fracture propagation and microearthquake production in hot pluton environments, J. Geophys. Res., 82, 2515-2522, 1977.

Meidav, T., and R. Furgerson, Resistivity studies of the Imperial Valley geothermal area, California, Geothermics, 1, 47-62, 1972.

Mitchell, B. J., and M. Landisman, Geophysical measurements in the southern great plains, in The Structure and Physical Properties of the Earth's Crust, Geophys. Monogr. Ser., vol. 14, edited by J. G. Heacock, pp. 77-95, AGU, Washington, D. C., 1971.

Moskowitz, B. M., Numerical analysis of electrical resistivity in hydrothermal systems, M.S. thesis, Univ. of Ariz., Tucson, 1977.

Norton, D., Fluid circulation in the earth's crust, in The Earth's Crust, Geophys. Monogr. Ser., vol. 20, edited by J. G. Heacock, in press, AGU, Washington, D. C., 1977.

Norton, D., and R. Knapp, Transport phenomena in hydrothermal systems: The nature of porosity, Amer. J. Sci., 277, 913-936, 1977.

Norton, D., and J. Knight, Transport phenomena in hydrothermal systems: Cooling plutons, Amer. J. Sci., 277, 937-981, 1977.

Norton, D., T. Gerlach, K. J. DeCook, and J. S. Sumner, Geothermal water resources in Arizona: Feasibility study, technical completion report, project A-054-ARIZ, Office of Water Res. and Technol., Tucson, Ariz., 1975.

Quist, A. S., and W. L. Marshall, Electrical conductances of aqueous sodium chloride solutions from 0°C to 200°C and at pressures to 4000 bars, J. Phys. Chem., 72, 684-703, 1968.

Risk, G. F., W. J. P. MacDonald, and G. B. Dawson, D. C. resistivity surveys of the Broadlands geothermal region, New Zealand, Geothermics, Spec. Issue, 2 (1), 287-294, 1970.

Sato, K., The present state of geothermal development in Japan, Geothermics, Spec. Issue, 2 (1) 155-184, 1970.

Shankland, T. J., and H. S. Waff, Conductivity in fluid-bearing rocks, J. Geophys. Res., 79, 4863-4868, 1974.

Zohdy, A. A. R., L. A. Anderson, and L. J. P. Muffler, Resistivity, self potential, and induced polarization surveys of a vapor-dominated geothermal system, Geophysics, 38, 1130-1144, 1973.

(Received March 15, 1977;
revised August 15, 1977;
accepted August 26, 1977.)

DOE/ID/12079-90
ESL-108

RESISTIVITY, INDUCED POLARIZATION, AND SELF-POTENTIAL METHODS IN GEOTHERMAL EXPLORATION

by

Stanley H. Ward
and
William R. Sill

Earth Science Laboratory
University of Utah Research Institute

and

Department of Geology and Geophysics
University of Utah

Work performed under contract DE-AC07-80ID12079

Prepared for
U.S. Department of Energy
Division of Geothermal Energy

ELECTRICAL PROPERTIES OF EARTH MATERIALS

Introduction

Bulk resistivities from the surface to in excess of 15 km depth in a normal crust are controlled by aqueous electrolytic conduction via pores, fractures, and faults. A slight increase in resistivity with depth in this region is the result of decreasing pore, fracture and fault porosity due to increased hydrostatic load. Fractures and faults are known to remain open to depths in excess of 5 km due to departures from hydrostatic loading. From about 15 km to the Moho, mineral semiconduction dominates and the resistivity decreases downwards. Semiconduction will remain the dominant conduction mechanism in excess of 100 km into the normal upper mantle.

In spreading centers (e.g. Iceland), intraplate melting zones (e.g. Hawaiian Islands), hot spots (e.g. Yellowstone, USA), subduction zones (e.g. Cascades volcanoes, USA and Canada), extensional continental regions (e.g. eastern Basin and Range, USA), and rift zones (e.g. East African Rift), the crust and mantle are abnormal in that they then contain melt or partial melt at any depth from surface to 100 km. Thus in geothermal areas, which abound in the tectonically active areas, one must be concerned with three basically different conduction mechanisms: aqueous electrolyte conduction, semiconduction, and melt conduction.

Aqueous Electrolyte Conduction

Normal mode of conduction

Conduction in near-surface rocks is largely electrolytic, taking place in pore spaces, along grain boundaries, in fractures and in faults but negligibly through the silicate framework.

The ions which conduct the current result from the dissociation of salts, such dissociation occurring when salts are dissolved in water. Since each ion is able to carry only a definite quantity of charge, it follows that the more ions that are available in a solution and the faster they travel, the greater will be the charge that can be carried. Hence, the solution with the larger number of ions will have the higher conductivity. Thus, in general, a rock which contains saline water within its pores will have a greater conductivity when the salinity of the water is high than when it is low; salinity is a major factor in determining the resistivity of a rock.

An increase in temperature lowers the viscosity of water, with the result that ions in the water become more mobile. The increased mobility of the ions results in an observed resistivity decrease with increase in temperature according to the formula

$$\rho_t = \frac{\rho_{18}}{1 + \alpha\,(t - 18)} \tag{34}$$

in which α is the temperature coefficient of resistivity (usually given as about 0.025 per degree centigrade), t is the ambient temperature, ρ_t is the resistivity at this temperature, while ρ_{18} is the resistivity at 18°C.

Archie's Law,

$$F = \frac{\rho_r}{\rho_w} = \phi^{-m}\,, \tag{35}$$

usually is satisfied for aqueous electrolytic conduction. In (35), F is formation factor, ρ_r is the resistivity of the rock, ρ_w is resistivity of the saturating electrolyte, ϕ is porosity, and m is

he cementation factor which usually varies between 1.5 and 3.

The effect of clays on rock resistivity

A clay particle acts as a separate conducting path additional to the electrolyte path. The resistance of this added path is low. The origin of this abnormally high clay mineral conductivity lies in the double layer of exchange cations as shown in Figure 1. The cations are required to balance the charge due to substitution within the crystal lattice, and to broken bonds (Grim, 1953). The finite size of the cations prevents the formation of a single layer. Rather, a *double layer* is formed; it consists of a *fixed layer* immediately adjacent to the clay surface and a *diffuse layer* which drops off in density exponentially with distance from the fixed layer.

The diffuse layer, in contrast to the fixed layer, is free to move under the influence of an applied electric field. The cations of the diffuse layer add to the normal ion concentration and thus increase the density of charge carriers. The net result is an increased *surface conductivity*. Although clay minerals exhibit this property to a high degree because of their large ion exchange capacity, all minerals exhibit it to a minor extent. All rocks containing clay minerals possess an abnormally high conductivity on this account.

The effect of disseminated clay or shale on rock resistivities becomes increasingly important as the conductance through the pores diminishes. In a geothermal environment, hydrothermal alteration converts feldspars to kaolinite,

montmorillonite and other clay minerals, especially in silicic rocks. In basic rocks, chlorite and serpentine may also be produced. All of these alteration products exhibit high surficial conductivity. As the concentration of the electrolyte increases, the relative contribution of the electrolyte conduction path to the clay conduction path increases as may be seen from the formula

$$\sigma_r = \frac{\sigma_e + \sigma_s}{F} \qquad (36)$$

in which σ_r, σ_e, and σ_s represent the observed conductivities of the rock, the electrolyte, and the clay surface path. Ward and Sill (1976) demonstrate that $\sigma_s \sim 3\ \sigma_e$ for altered rocks at Roosevelt Hot Springs, Utah, USA, despite the presence of an electrolyte containing 7000 ppm total dissolved solids.

Induced Polarization in Geothermal Areas

Introduction

Pyrite and clay minerals often are found as alteration products in geothermal areas. Hence the induced electrical polarization mechanisms of electrode polarization and membrane polarization might be expected in these areas.

Electrode polarization

Whenever there is a change in the mode of current conduction, e.g. from ionic to metallic, energy is required to cause the current to flow across the interface. This energy barrier can be considered to constitute an electrical impedance.

The surfaces of most solids possess a very small net attraction for either cations or anions, as we mentioned earlier for

clay minerals. Immediately adjacent to the outermost solid layer is adsorbed a layer of essentially fixed ions, one or a few molecular layers in thickness (Figure 2a). These are not truly exchangeable and, hence, constitute the fixed layer.

Adjacent to the fixed layer of adsorbed ions there is a group of relatively mobile ions, either of the same or opposite charge, known as the diffuse layer. The *anomalous* number of ions in this zone decreases exponentially from the fixed layer outward to the normal ion concentration of the liquid. (The normal balanced distribution of anions and cations has been deleted from Figure 2 for clarity). The particular distribution of ions shown is only one of several possible distributions, but it is the most common. The electrical potential across the double layer has been plotted also; the potential drop across the diffuse layer is known as the Zeta potential (Z).

While the fixed layer is relatively stable, the diffuse layer thickness is a function of temperature, ion concentration in the *normal* electrolyte, valency of the ions, and the dielectric constant of the medium. Most of the anomalous charge is contained within a plane distance d from the surface, where (Grahame, 1947)

$$d = \left[\frac{\epsilon_o K_e k T}{2ne^2v^2}\right]^{1/2}, \qquad (37)$$

n = normal ion concentration of the electrolyte,

v = valence of the normal ions,

e = elementary charge,

K_e = the dielectric constant of the medium,

k = Boltzman's constant,

and

T = temperature.

The thickness is, therefore, governed by the balance between the attraction of unlike charges at the solid surface and the thermal redistribution of ions. Obviously, increasing n, the salinity, or v, the valence, decreases the diffuse layer thickness.

Returning now to polarization at electrodes, it may be stated that there are two paths by which current may be carried across an interface between an electrolyte and a metal (Figure 3). These are called the faradaic and nonfaradaic paths. Current passage in the faradaic path is the result of an electrochemical reaction such as the oxidation or reduction of some ion, and may involve the diffusion of the ions toward or away from the interface. The charge is carried physically across the interface by an electron transfer. In the latter, i.e. nonfaradaic, case, charged particles do not cross the interface; rather, current is carried by the charging and discharging of the double layer. The nonfaradaic component, thus, may be represented by a simple capacitance insofar as the variation of its impedance with frequency is concerned.

In the faradaic path, the impedance associated with the electron transfer is represented by the reaction resistance. The ion diffusion process is not representable in so simple a fashion and, in fact, may not be adequately represented by any combination of fixed capacitors and resistors. It is customarily referred to as the Warburg impedance W and its magnitude varies inversely with the

square root of the electrical frequency.

The interfacial impedances of many metal-electrolyte interfaces may be described roughly as follows. Above 1,000 Hz the major part of the electric current is carried across the interface by means of the non-faradaic path; hence, the interfacial impedance varies with frequency as approximately f^{-1}. As the frequency is lowered, more and more current is carried via the faradaic path, and so the low frequency impedance varies with frequency in the range $f^{-1/2}$ to f^{0} depending on the magnitude of the impedance ratio W/R.

All of the above discussion applies to an ideal electrode in a pure electrolyte. The concepts, however, are important in understanding the processes occurring when current is passed through a rock. Any rock sample is *dirty* from the viewpoint of the physical chemist since the electrodes (metallic mineral grains) and electrolytes (pore solutions) are anything but pure. Nevertheless we perhaps are justified in employing equivalent circuits based on pure systems since a phenomenological explanation for rock behavior results. With this caution, one might suggest the equivalence of the elementary rock system of Figure 4a with the equivalent circuit of Figure 4b, where

W is the Warburg impedance

[= $k(1 - i)/ f^{1/2}$; k is a constant],

C_F is the double layer capacitance,

C_{CH} is the chemical capacitance,

R is the reaction resistance,

R' is the resistance representing a higher order reactions,

R_i is the resistance of ionic path,

and

R_m is the resistance of metallic vein path or particle.

In noting these circuit elements, it must be appreciated that one chemical reaction at the interface may lead to a chain of subsequent reactions involving electrons, ions, and molecules of all reaction products present. At each point of the reaction chain, the accumulation of the reaction product represents a capacitance C_{CH} to the electrode. The escape of the product is achieved either by diffusion, represented by a Warburg impedance W, or by a reaction represented by a resistor R. The product of this reaction in turn follows a similar circuit behavior which we have omitted for simplicity, except to lump all such products as R'.

While the circuits of Figure 4b and 4c satisfy the expected physical/chemical processes in mineralized rock, they are too complicated for practical use. Thus, the simple circuit of Figure 5a is used to predict induced polarization, of both electrode and membrane type, in a rock. The frequency and time domain responses of the circuit of Figure 5a are shown in Figures 5b and 5c, respectively. This is the Cole-Cole model of relaxation used by Pelton et al. (1978).

Membrane polarization.

In rocks containing a few percent clays distributed throughout the rock matrix, membrane polarization is of importance. Membrane polarization arises chiefly in porous rocks in

which clay particles (membranes) partially block ionic solution paths [Figure 6a]. The diffuse *cloud* of cations (double layer) in the vicinity of a clay surface is characteristic of clay-electrolyte systems. On application of an electrical potential, positive charge carriers easily pass through the cationic cloud but negative charge carriers accumulate [Figure 6b]; an ion-selective membrane, therefore, exists.

Consequently, a surplus of both cations and anions occurs at one end of the membrane zone, while a deficiency occurs at the other end. This is because the number of positive charges cannot deviate significantly from the number of negative charges at any one point in space due to the large electric fields which would result if they did so deviate. These ion concentration gradients oppose the flow of current. The overall mobility of ions is reduced by this process. This reduction in mobility is most effective for potential variations which are slow (e.g., 0.1 Hz) with respect to the time of diffusion of ions between adjacent membrane zones. For potential variations which are fast (e.g., 1,000 Hz) with respect to the diffusion time, the mobility of ions is not substantially reduced. Hence, the conductivity of a membrane system increases as electrical frequency increases.

Semiconduction

The *intrinsic* conductivity of a solid at temperature T is computed from the relation

$$\sigma = |e| \left[n_e \mu_e + n_h \mu_h\right] \tag{38}$$

where n_e, n_h are the electron and hole equilibrium concentrations, and μ_e, and μ_h are the mobilities of electrons and holes respectively while e is the elemental charge.

Kinetic theory leads us to expect a temperature dependence of the form $e^{-E/kT}$ for the concentration of electrons in the conduction band of a solid. Assuming a relatively small variation of mobility with temperature, we are then led (Kittel 1953) to predict a conductivity dependence of the form

$$\sigma = \sigma_o e^{-E_g/2kT} \tag{39}$$

in which E_g is the gap energy, σ_o includes the mobility function, and, in this form, is the conductivity as $T \to \infty$. Boltzmann's constant is k. Thermal, electrical, or optical excitation of electrons across the band of forbidden energy renders the solid conducting.

Impurities and imperfections in the material produce extrinsic conductivity. Above some temperature, impurities may be unimportant so that we define the temperature range above extrinsic conductivity as the intrinsic range in which the previous mechanism is operative.

However, below the intrinsic range, certain types of impurities and imperfections markedly alter the electrical properties of a semiconductor. Extrinsic semiconduction arises by the thermal excitation of electrons (occupying intermediate energy levels in the forbidden gap produced by impurities in solid solution) into the unoccupied conduction band, or by the excitation of electrons from the occupied valence band into unoccupied impurity levels.

Ionic conduction in a solid occurs as a result of mobile ions moving through the crystal lattice as a result of defects in it. The simplest imperfection is a missing atom or lattice vacancy (Schottky defect). The diffusion of the vacancy through the lattice constitutes transport of charge. The conduction mechanism above 1,100°C is recognized as ionic because, when an iron electrode is used in contact with a magnesium orthosilicate, iron diffuses into the silicate replacing the magnesium.

Table 1 illustrates the temperature ranges important to extrinsic, intrinsic, and ionic conduction.

Melt Conduction

A silicic magma chamber can be expected to exhibit a resistivity two to three orders of magnitude lower than its solid rock host as the experiments of Lebedev and Khitarov (1964) have demonstrated. Duba and Heard (1980) measured resistivity on buffered olivene while Rai and Manghnani (1978) measured electrical conductivity of basalts to 1550°C; these latter measurements establish that mafic rocks can demonstrate low resistivities also. Resistivities of order 1 Ω m are to be expected in either silicic or basic melts due to ionic conduction.

For partial melts, the melt phase will serve as an interconnection of low resistivity in a residual crystal matrix of resistivity two or more orders greater and will determine the bulk resistivity (Shankland and Waff, 1977). An Archie's Law dependence is hence expected.

FIGURE CAPTIONS

Fig. 1. Schematic representation of ions adsorbed on clay particle (after Ward and Fraser, 1967).

Fig. 2. (a) Hypothetical anomalous ion distribution near a solid-liquid interface; (b) Corresponding potential distribution (after Ward and Fraser, 1967).

Fig. 3. Circuit analog of interfacial impedance (after Ward and Fraser, 1967).

Fig. 4. Simplified representation of mineralized rock, (a) and the corresponding equivalent circuit (b) and (c) equivalent circuit of all mineralized rocks (after Ward and Fraser, 1967).

Fig. 5. Simplified analog circuit model of rock. (a) Elementary circuit, (b) frequency response of elementary circuit, (c) transient response of elementary circuit, and (d) a generalization of the elementary circuits.

Fig. 6. Depiction of ions in a pore space forming an ion concentration barrier which creates membrane polarization: (a) Pore path before application of an electric potential, (b) Pore path after application of a potential (after Ward and Fraser, 1967).

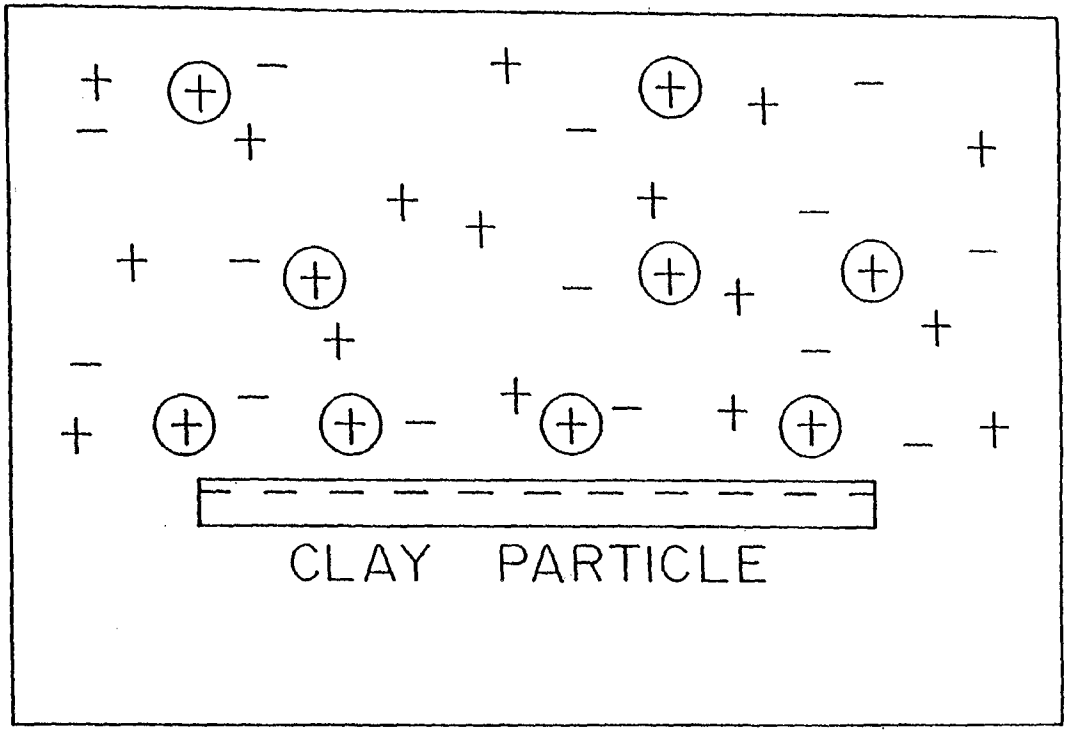

⊕ ADSORBED AND EXCHANGE CATIONS
\+ NORMAL CATIONS
− NORMAL ANIONS

Fig. 1. Schematic representation of ions adsorbed on clay particle (after Ward and Fraser, 1967).

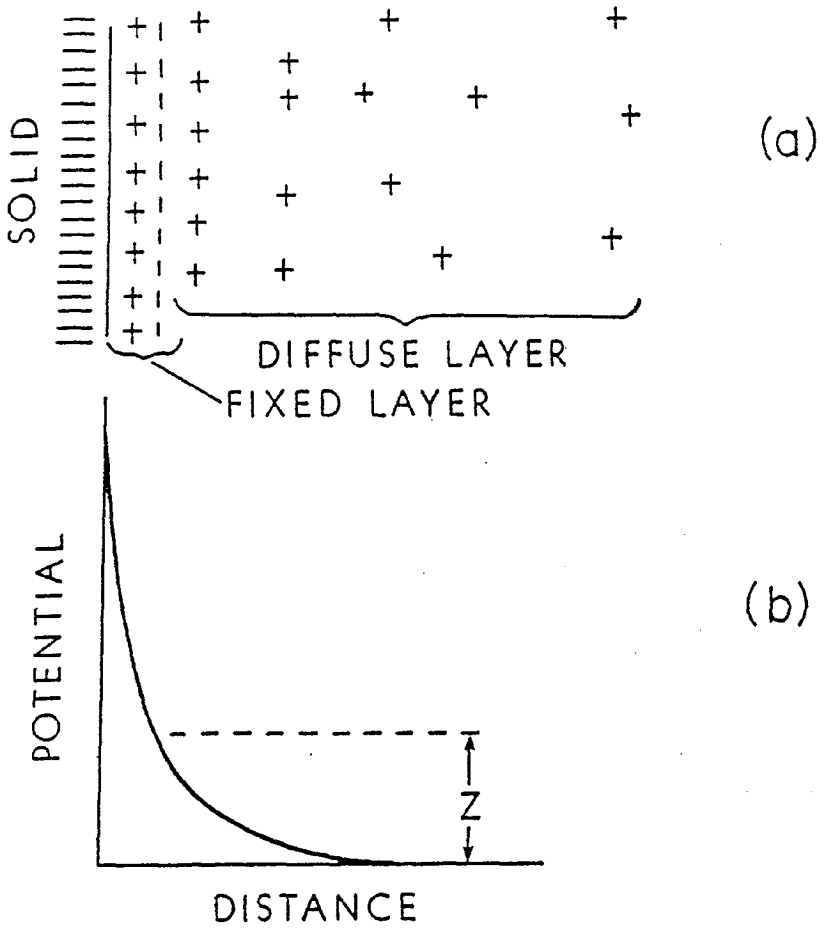

Fig. 2. (a) Hypothetical anomalous ion distribution near a solid-liquid interface; (b) Corresponding potential distribution (after Ward and Fraser, 1967).

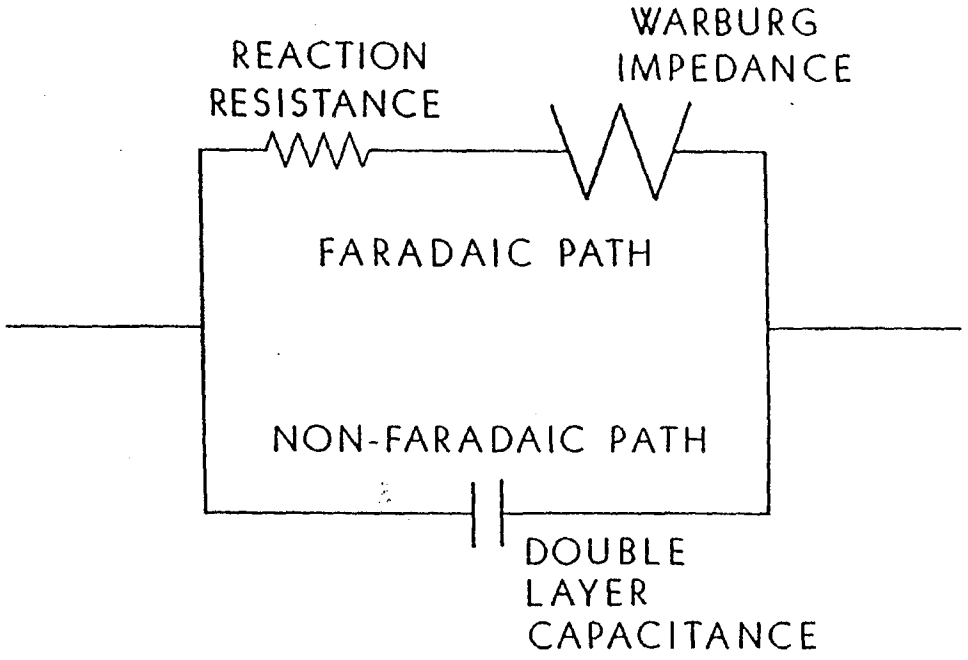

Fig. 3. Circuit analog of interfacial impedance (after Ward and Fraser, 1967).

ANALOG CIRCUIT MODEL OF ROCK

a) ELEMENTARY CURCUIT

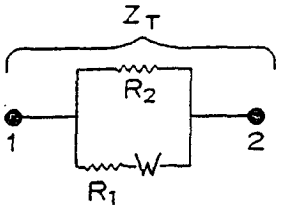

$$Z_2 = \frac{R_1 + W}{1 + \frac{R_1}{R_2} + \frac{W}{R_2}}$$

b) FREQUENCY RESPONSE - SINE WAVE EXCITATION

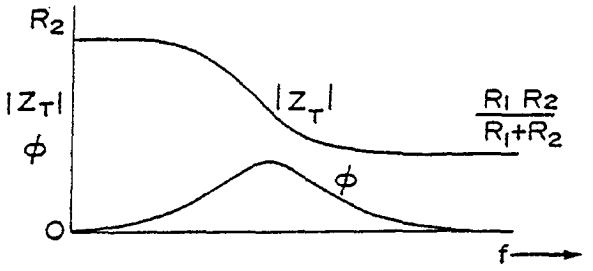

c) TRANSIENT RESPONSE SQUARE WAVE EXCITATION

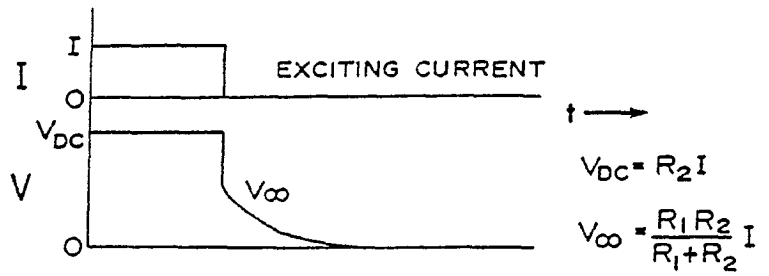

Fig. 5. Simplified analog circuit model of rock. (a) Elementary circuit, (b) frequency response of elementary circuit, (c) transient response of elementary circuit, and (d) a generalization of the elementary circuits.

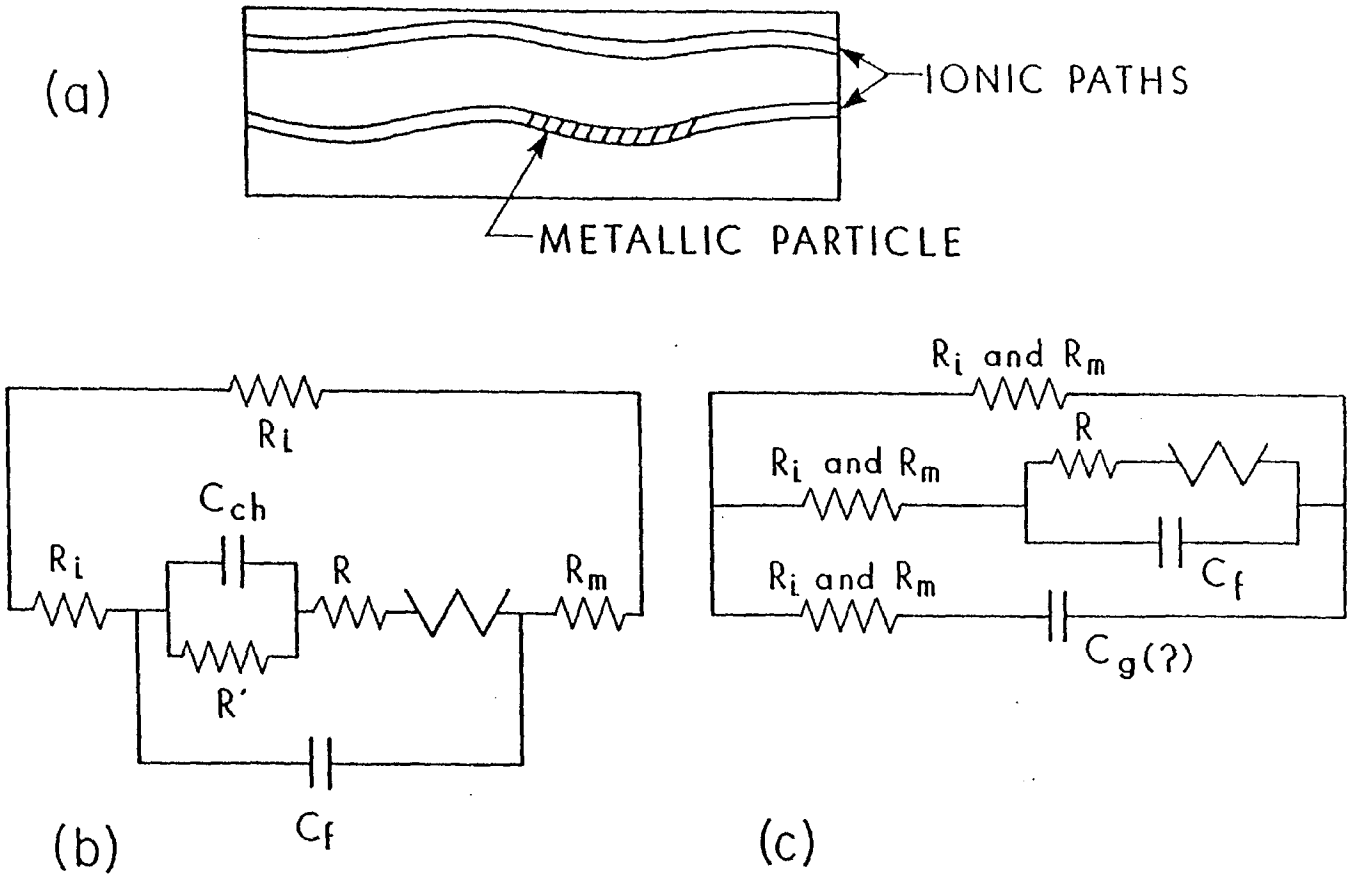

Fig. 4. Simplified representation of mineralized rock, (a) and the corresponding equivalent circuit (b) and (c) equivalent circuit of all mineralized rocks (after Ward and Fraser, 1967).

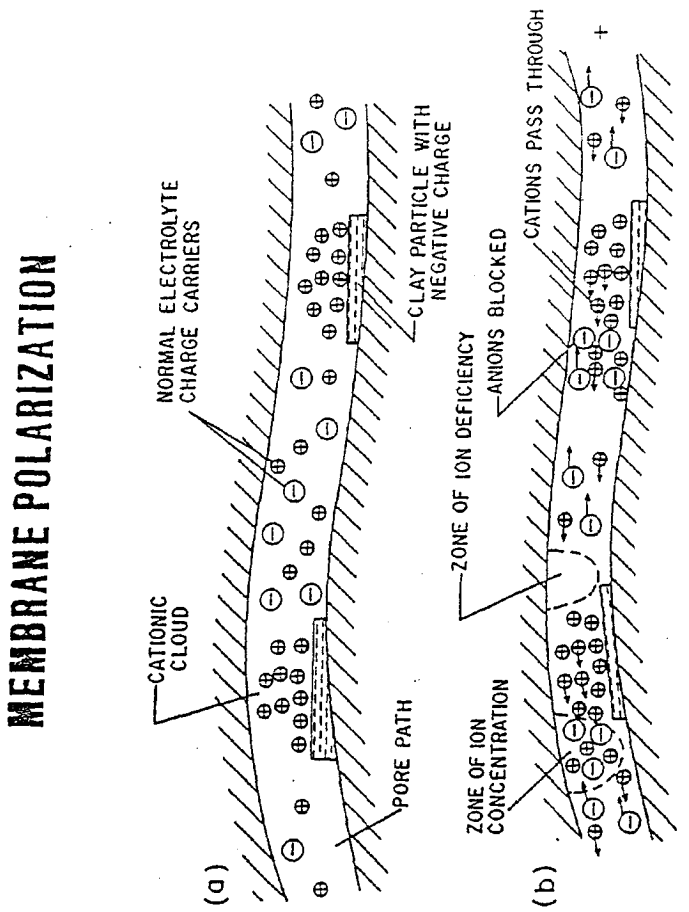

Fig. 6. Depiction of ions in a pore space forming an ion concentration barrier which creates membrane polarization: (a) Pore path before application of an electric potential, (b) Pore path after application of a potential (after Ward and Fraser, 1967).

TABLE 1

TYPE OF SEMICONDUCTION	σ_o	E	RANGE OF IMPORTANCE
EXTRINSIC	10^{-6} mho/m	1 ev	600°C
INTRINSIC	10^{-3} mho/m	3.3 ev	600 to 1,100°C
IONIC	10^{3} mho/m	3.0 ev	1,100°C

Table 1 Semiconduction follows the formula $\sigma=\sigma_0 e^{-E/kT}$ but σ_0 and E are different for each conduction mechanism. The values of σ_0 and E are stated here as are the temperature ranges of importance to each of the three mechanisms; extrinsic electronic, intrinsic electronic and ionic.

ELECTROMAGNETIC PROPERTIES OF ROCKS

by

William R. Sill

The electromagnetic properties of rocks appear in the constitutive relationships for the field vectors of Maxwell's equations. The constitutive equations are

$$B = \mu \cdot H \,, \tag{1}$$

$$D = \varepsilon \cdot E \,, \tag{2}$$

and

$$J = \sigma \cdot E \,, \tag{3}$$

where μ is the magnetic permeability, ε is the dielectric permittivity and σ is the electrical conductivity. In general, the relations in equations (1) to (3) can be nonlinear and the constitutive parameters are complex tensors which can be functions of frequency (time), temperature, pressure and composition. Under the more usual conditions they are treated as real or complex constants.

Measurements of these parameters are often carried out by forming the sample into a convenient geometry and measuring the capacitance, inductance, and resistance of the sample. Under the appropriate assumptions these measurements and the known geometry can be used to calculate the intrinsic values of the dielectric constant $(\varepsilon/\varepsilon_0)$, the relative magnetic permeability (μ/μ_0) and the electrical conductivity or resistivity $(\rho = 1/\sigma)$. The interpretations of laboratory measurements of these properties is not always as straightforward as the above discussion might indicate. Certain interfacial effects that can occur at the boundaries of the sample can invalidate the interpretation and steps must be taken to reduce them. Electrode polarization in dielectric and conductivity measurements is an important example of these effects. Also in the case of electrical measurements, dielectric effects can be superimposed on conduction effects and this can complicate the interpretation.

Another approach to the description of electromagnetic properties involves the use of mixture formulas for heterogeneous systems. These are usually developed in conjunction with laboratory measurements of the properties and they often present a useful insight into the physical processes involved. In a rock the heterogeneous system consists of the rock forming minerals and the material filling the pore space. The pore filling is usually a water solution or less often a gas or a liquid hydrocarbon. In a rock, the contributions of the various components differ widely depending on the property and the physical conditions as we shall see in the following discussions.

Magnetic Permeability

In rocks the principal magnetic minerals and their permeabilities are given in Table 1.

Table 1

Magnetic Minerals

Mineral	μ/μ_0
Magnetite	5
Pyrrhotite	2.6
Ilmenite	1.6
Hematite	1.05
Pyrite	1.0015

Except for massive orebodies, these minerals are usually minor constituents of rocks. A useful mixing law for rocks expresses the relative magnetic permeability (μ_r) as

$$\mu_r = 1 + (\mu_m - 1)v_m$$

where μ_m is the relative magnetic permeability of the magnetic mineral and v_m is its fractional volume. For one percent magnetite in a granite the relative magnetic permeability is around 1.04. In most electromagnetic prospecting problems it is therefore assumed that the magnetic permeability is the same as free space.

Dielectric Constant

The dielectric constant ($\varepsilon/\varepsilon_0$) of most rock forming silicates falls in the range from 1 to 10. The next most important constituent is water with a low frequency dielectric constant of about 80 (Figure 1). Small amounts of adsorbed water on the pore surfaces of nominally "dry" rocks can have profound and complicated effects on the electrical properties because the interfacial water is conductive and polarizable. Under terrestrial conditions where the more usual saturation is in the range from a few percent to completely saturated, the effects of the water become more tractable since the conduction and dielectric polarization in the bulk pore water dominate over the interfacial region. True dielectric measurements are usually made at relatively high frequency ($> 10^4$ hertz) first to minimize electrode polarization effects and second to ensure that displacement current is a dominant or at least a significant mechanism. When the effects of the interfacial water layers and the effects of conducting minerals in the rock can be ignored a useful formula for the dielectric constant (K_r) is given by the geometric mixing law,

$$K_r = \pi_i K_i^{v_i}, \qquad (1)$$

where K_i is the dielectric constant of the i^{th} component and v_i is its volume fraction. In a typical rock with an average silicate dielectric constant of 5, containing 10 percent water, the rock dielectric constant is about 7.

Measured values on rocks fall in the range from around 4 to 25 (Telford et al., 1976).

Electrical Conductivity

The electrical conductivity of most silicates is very small ($< 10^{-9}$ s/m) at room temperature while the conductivity of pore water is much larger, usually in the range from 10^{-3} to 10^{1} s/m. Under the usual upper crustal conditions the pore water exists as an interconnected network and the conductivity of rocks is controlled solely by the conductivity of the pore water and the conductivity of the pore water-silicate interface. When the bulk pore water conduction dominates a useful mixing formula is given by Archie's law,

$$\sigma_r = \sigma_w \phi^m , \qquad (2)$$

where σ_r is the rock conductivity, σ_w is the pore water conductivity and ϕ is the functional porosity of the interconnected pore spaces. The exponent m is sometimes referred to as the cementation index and it has a value in the range from 1 to 3 depending on the rock type. Usually larger values for m are associated with "tighter" rocks and low porosity. The effects of the geometry of the pore network can be combined into the formation factor (F) which is given by

$$F = \phi^{-m} . \qquad (3)$$

The remaining factor determining the rock conductivity is then the conductivity of the pore water which can be expressed as,

$$\sigma_w = \sum_i n_i Z_i e U_i \qquad (4)$$

where n_i is the concentration of the i^{th} ion, Z_i is its valence, e is the

electronic charge and U_i is the mobility. The mobility of most ions in water solutions is similar ($U \sim 5 \times 10^{-8}$ $m^2 S^{-1} V^{-1}$) so that the major factor affecting the conductivity is the concentration. The mobility of ions in solution is dependent on the temperature and this effect can be incorporated into the conductivity as

$$\sigma_r(T) = \sigma_r(T_0)[1 + \alpha (T - T_0)] \qquad (5)$$

where T_0 is the reference temperature and the temperature coefficient α is around $0.025°C^{-1}$. At higher temperatures the dependence is nonlinear similar to the change in viscosity. At temperatures near the triple point, the conductivity starts to decrease with temperature (Figure 2). This decrease is mostly due to an increase in ion association caused by the rapidly decreasing dielectric permittivity.

Interfacial effects on the conductivity arise because of the excess charge in the electrical double layer at the pore water-silicate interfaces (Figure 3). At most silicate interfaces the interaction with an electrolyte of moderate pH leads to a net negative charge on the interface and a compensating net positive charge in the diffuse portion of the double layer. With clay-type silicates the most important effect results from a net negative charge in the clay lattice and a compensating positive charge of exchange cations in the diffuse layer. In either case, the excess charge in the diffuse layer is relatively free to move under the influence of an electric field and this movement gives rise to the surface conductivity. The mobility of these ions is not as large as that of the same ions in a bulk solution and the temperature dependence is somewhat different (Waxman and Smits, 1968; Waxman and Thomas, 1974). The Waxman-Smits model provides a useful equation to describe the combined bulk and surface effects. This equation can be

written as

$$\sigma_r = F^{-1}(\sigma_w + \sigma_s) \ , \tag{6}$$

where σ_s is the contribution from the surface conduction. For clay minerals in sedimentary rocks Waxman and Smits (1968) give the surface conductivity as

$$\sigma_s = B\ Q_v \ , \tag{7}$$

where B is the mobility of the clay exchange ions and Q_v is the cation exchange capacity per unit pore volume. When Q_v is express in equivalents per liter, which is a measure of the average concentration of the exchange ions in the pore volume, B is given by

$$B = 3.83\ (1 - .83\ \exp(-2\sigma_w)) \ , \tag{8}$$

where σ_w is expressed in s/m. Equation (9) shows that the mobility in the Waxman-Smits model is an increasing function of the pore water conductivity.

A similar model for the surface effects due to non-clay silicates (Sill, 1982) gives σ_s as

$$\sigma_s = 2q^*\ U^*\ S_v \ , \tag{9}$$

where q^* is the charge in the diffuse layer, U^* is the mobility of these ions and S_v is the surface area to volume ratio.

The major difference between the clay and normal silicate interface is the much larger surface charge on the clay. The charge density on montmorillonite is about 10^{-1} coulomb/m^2 while for a silicate with a surface potential of about 50 mV in a solution of concentration 10^{-2} molar the surface charge would be about 10^{-2} coulombs/m^2.

Semiconduction

The *intrinsic* conductivity of a solid at temperature T is computed from the relation

$$\sigma = |e| [n_e \mu_e + n_h \mu_h] \tag{10}$$

where n_e, n_h are the electron and hole equilibrium concentrations, and μ_e and μ_h are the mobilities of electrons and holes respectively while e is the elemental charge.

Kinetic theory leads us to expect a temperature dependence of the form $e^{-E/kT}$ for the concentration of electrons in the conduction band of a solid. Assuming a relatively small variation of mobility with temperature, we are then led (Kittel 1953) to predict a conductivity dependence of the form

$$\sigma = \sigma_0 e^{-E_g/2kT} . \tag{11}$$

in which E_g is the gap energy, σ_0 includes the mobility function, and, in this form, is the conductivity as $T \to \infty$. Boltzmann's constant is k. Thermal, electrical, or optical excitation of electrons across the band of forbidden energy renders the solid conducting.

Impurities and imperfections in the material produce extrinsic conductivity. Above some temperature, impurities may be unimportant so that we define the temperature range above extrinsic conductivity as the intrinsic range in which the previous mechanism is operative.

However, below the intrinsic range, certain types of impurities and imperfections markedly alter the electrical properties of a semi-conductor. Extrinsic semiconduction arises by thermal excitation of electrons (occupying

intermediate energy levels in the forbidden gap produced by impurities in solid solution) into the unoccupied conduction band, or by the excitation of electrons from the occupied valence band into unoccupied impurity levels.

Ionic conduction in a solid occurs as a result of mobile ions moving through the crystal lattice as a result of defects in it. The simplest imperfection is a missing atom or lattice vacancy (Schottky defect). The diffusion of the vacancy through the lattice constitutes transport of charge. The conduction mechanism above 1,100°C is recognized as ionic because, when an iron electrode is used in contact with a magnesium orthosilicate, iron diffuses into the silicate replacing the magnesium.

Table 2 illustrates the temperature ranges important to extrinsic, intrinsic, and ionic conduction.

Table 2

Values for the constants in equation (11) and the temperature region where the mechanism is important.

Conduction Mechanism	σ_0(s/m)	E_g(eV)	Range of Importance
Extrinsic	10^{-6}	1.0	600°C
Intrinsic	10^{-3}	3.3	600°-1100°C
Ionic	10^{3}	3.0	1100°C

Melt Conduction

A silicic magma chamber can be expected to exhibit a resistivity two to three orders of magnitude lower than its solid rock host as the experiments of Lebedev and Khitarov (1964) have demonstrated. Duba and Heard (1980) measured resistivity on buffered olivene where Rai and Manghnani (1978) measured electrical conductivity of basalts to 1550°C; these latter measurements establish that mafic rocks can demonstrate low resistivities also.

Resistivities of order 1 Ω m are to be expected in either silicic or basic melts due to ionic conduction.

For partial melts, the melt phase will serve as an interconnected phase of low resistivity in a residual crystal matrix of resistivity two or more orders greater. This situation is similar to ordinary electrolytic conduction and an Archie's Law dependence is expected (Shankland and Waff, 1977).

Summary

The previous discussions have concentrated on the real part of the material property, treating them as scalar constants. This treatment is an oversimplification but the objective was to illustrate the major factors controlling the gross electromagnetic properties of rocks. In the case of induced polarization this treatment is inadequate and the details of this phenomena will be addressed later.

The treatment of the magnetic permeability is the simplest. Usually the permeability is taken to be that of free space unless the earth contains massive amounts of magnetic minerals.

The dielectric constant of saturated rocks is also relatively simple to treat when the effects due to the polarization of the adsorbed water can be neglected. The contribution of the dielectric displacement current ($\omega\epsilon E$) relative to the conduction current (σE) can be evaluated by a consideration of the total current (J_T) given by

$$J_T = \sigma E + i\,\omega\epsilon E \,. \qquad (12)$$

The ratio of the displacement current to the conduction current is then

$$\frac{\omega\epsilon}{\sigma} = 10^{-10}\,\frac{\varepsilon}{\varepsilon_0}\frac{\rho}{\sigma} \,. \qquad (13)$$

Since the typical dielectric constant is about 10, the displacement current is relatively unimportant for frequency below a megahertz when the conductivity is larger than 10^{-2} s/m.

In the treatment of the conductivity the major factors were shown to be the water content, the geometry of the water network, the conductivity of the pore water and the surface conductivity. Surface conduction depends on the amount of clay present or the pore surface area to volume ratio for non-clay silicates. In both cases the surface conduction can become unimportant if the pore water conductivity is large enough.

The porosity of rocks can vary from a few tenths of a percent to around fifty percent giving rise to formation factors which span the range from 10^{-4} to almost 10^{0}. Since the conductivity of pore water ranges from 10^{-3} to 10^{1} s/m, it is not surprising that the observed range of rock conductivity in the upper crust is from 10^{-5} to 10^{1} s/m.

As rocks are subjected to greater lithostatic loading with depth, the porosity decreases. In the study of this decrease in porosity it is useful to separate the porosity into various categories depending on size and geometry. At the small end of the scale there are pores (rounded or tubular openings) and micro-cracks (thin and somewhat planar) and at the large end there are macro-cracks such as joints and fractures. The closing of these large scale joints and fractures with depth has been estimated by Brace (1971) to occur at depths of the order of hundreds of meters. However, we should probably discriminate between these types of fractures and joints and fault zones which are known to be open and permeable to much greater depths. For small scale features the laboratory studies of Brace and his co-workers (Brace et al, 1965; Brace and Orange, 1968; Brace, 1971) have shown the effects that

crack and pore porosity have on the conductivity of rocks. In general the crack porosity can be an important contribution at low pressures where the cracks are largely open. At pressures above a few killobars most of the cracks close and the remaining porosity is due mostly to the more equidimensional pores. As the cracks close in the low pressure region the conductivity may decrease by an order of magnitude in a few killobars. At higher pressures, the rate of decrease due to pore closure levels off to about ten percent per killobar. Effective pressures of a few killobars correspond to depths in the range from 5 to 10 killometers so the rapid change in conductivity due to crack closure is expected to take place in this depth range. In the crust temperature also increases with depth and this will initially lead to an increase in the water conductivity. However, the decrease in porosity can usually be expected to be large enough that the net effect is a decrease in conductivity. At still greater depths and temperatures solid state semiconduction in the silicate framework will ultimately lead to an increase in the conductivity. These effects are illustrated in the models in Figure 4 from Brace (1971). The initial decrease in conductivity at essentially zero depth is due to the closure of large scale joints and fractures and the next region of rapid decrease which extends to about 8 killometers is due to the closure of micro-cracks. Below 8 killometers the more gradual decrease is due to the closure of pores and finally the rapidly increasing conductivity is due to the contribution from solid state semiconduction.

REFERENCES

Brace, W. F., Orange, A. S., and Madden, T. R., 1965, The effect of pressure on the electrical resistivity of water-saturated crystalline rocks: J. Geophys. Res., v. 70, p. 5669-5678.

Brace, W. F., and Orange, A. S., 1968, Further studies of the effect of pressure on the electrical resistivity of rocks: J. Geophys. Res., v. 73, p. 5407-5420.

Brace, W. F., 1971, Resistivity of saturated crustal rocks to 40 km based on laboratory measurements: in AGU Geophysical Monograph 14, p. 243-256.

Duba, A., and Heard, H. C., 1980, Effect of hydration on the electrical conductivity of olivine: EOS transactions, 61, p. 404.

Kittel, C., 1953, Introduction to solid state physics: John Wiley and Sons, New York, 617 p.

Lebedev, E. B., and Khitarov, N. I., 1964, Dependence of the beginning of melting in granite and the conductivity of its melt on high water vapor pressure: Geokhimija, 3, p. 195-201.

Rai, C. S., and Manghnani, M. H., 1978, Electrical conductivity of basalts to 1550°C: in Proc. of Chapman Conference on Partial Melting in the Upper Mantle, Oregon Dept. of Geol. and Min. Ind., Bull. 96, p. 219-232.

Shankland, T. J., and Waff, H. S., 1977, Partial melting and electrical conductivity anomalies in the upper mantle: J. Geophys. Res., v. 82, p. 5409-5417.

Sill, W. R., 1982, A model for the cross-coupling parameters of rocks: Univ. of Utah, Dept. of Geol. and Geophys., DOE/DGR Report No. DOE/ID/12079-69.

Telford, W. M., Geldart, L. P., Sheriff, R. E., and Keys, D. A., 1976, Applied Geophysics: Cambridge Univ. Press, New York.

Waxman, M. H., and Smits, L. J. M., 1968, Electrical conductivities of oil-bearing shaly sands: Soc. Pet. Eng. J., v. 8, p. 107-172.

Waxman, M. H., and Thomas, E. C., 1974, Electrical conductivities in shaly sands: J. Pet. Tech., Feb., p. 213-225.

List of Figures

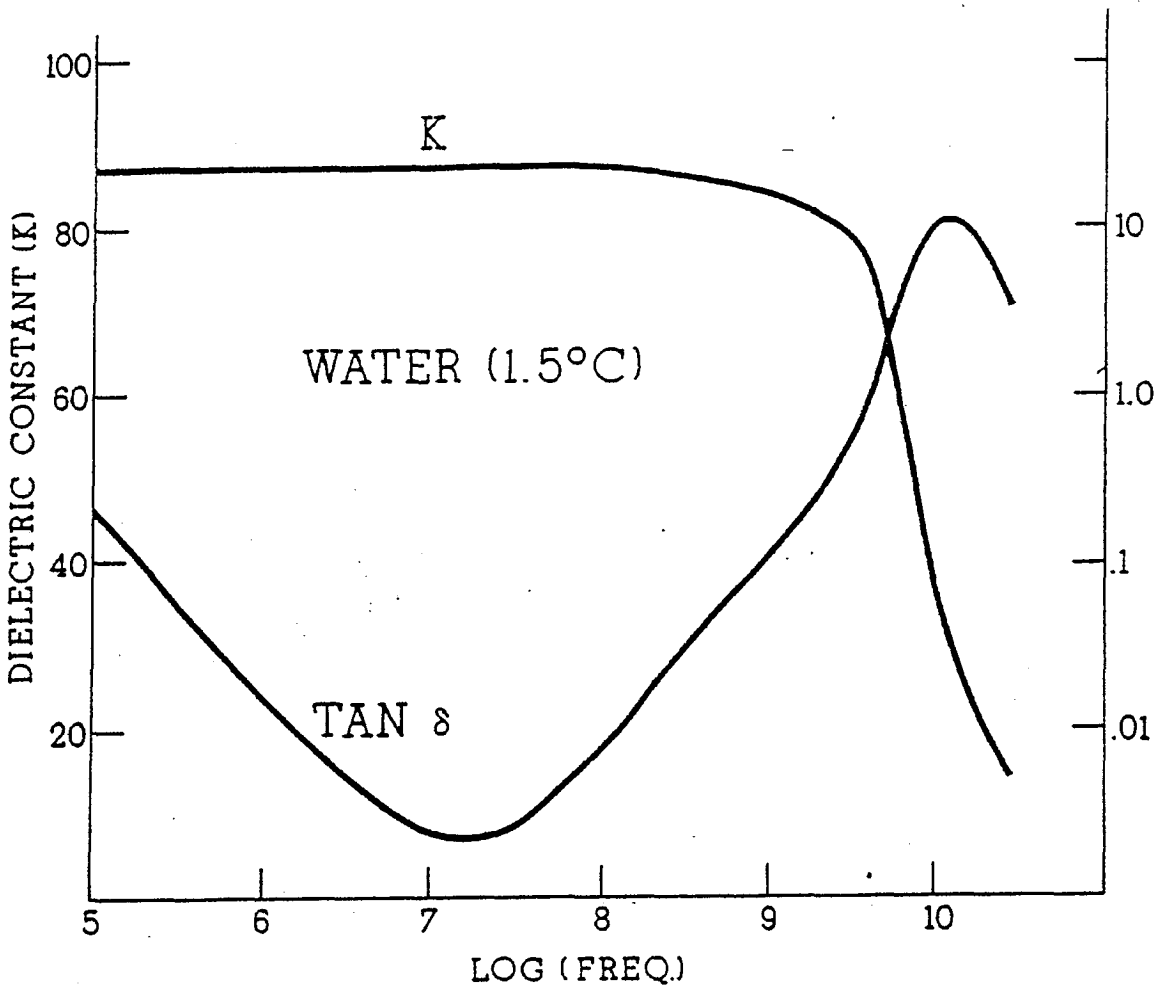

Figure 1. Dielectric constant (K) and loss tangent (Tan δ) of water.

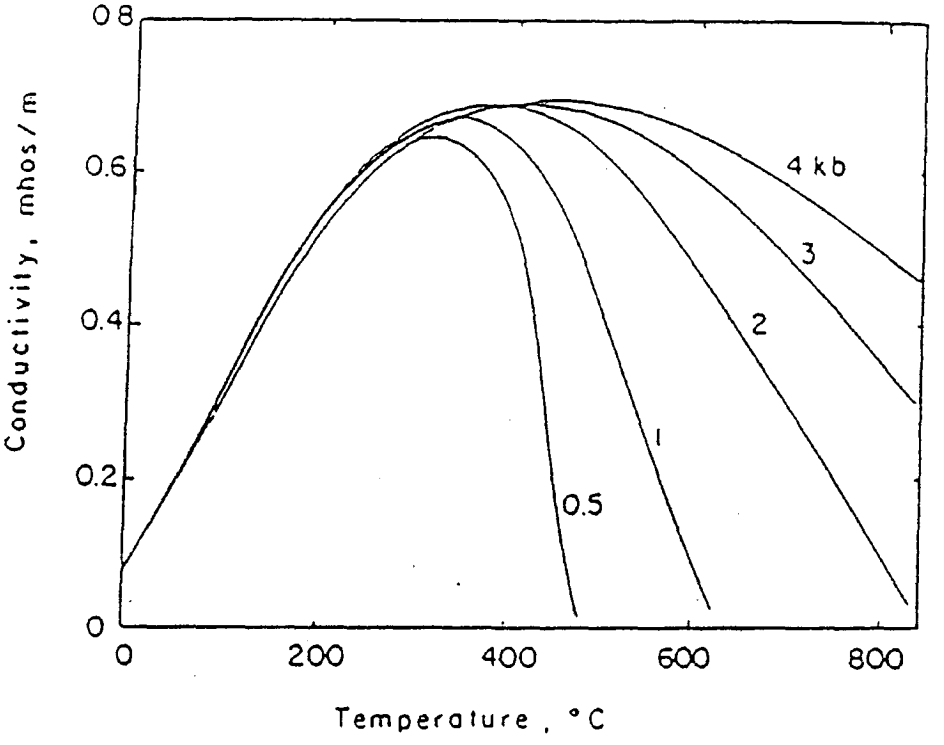

Figure 2. Conductivity of 0.01 molar NaCl as a function of temperature. The number on each curve is P_{H_2O}. (Quist and Marshall, 1968).

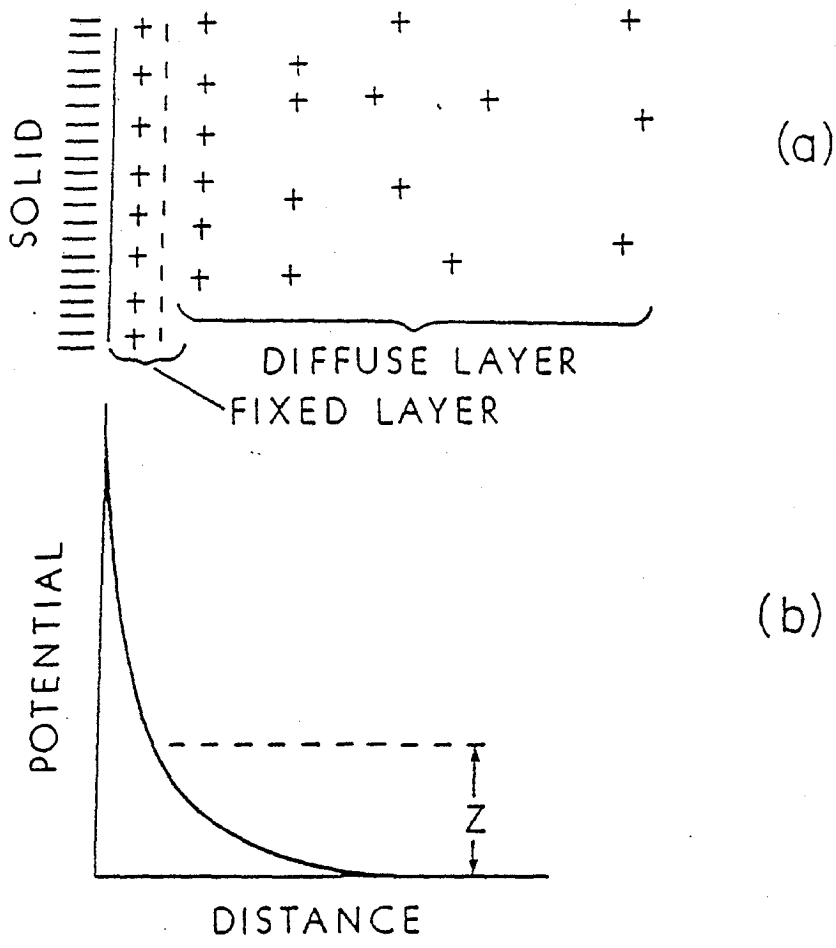

Figure 3. a) Ion distribution near a solid-liquid interface;
b) Corresponding potential distribution. (Ward and Fraser, 1967).

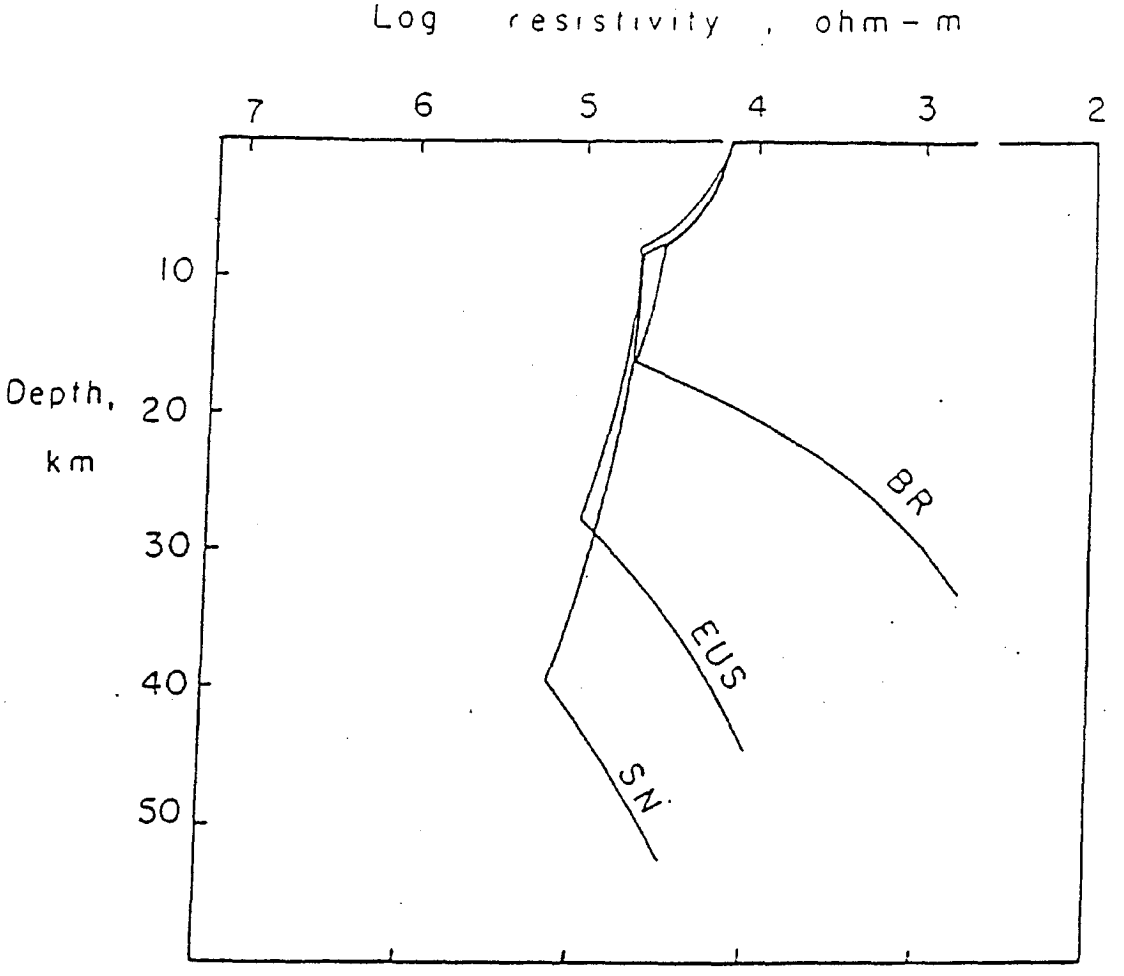

Figure 4. Comparison of resistivity-depth profiles for three heat flow provinces. (Brace, 1971).